Pergamon

Tetrahedron 58 (2002) 2861–2874

TETRAHEDRON

The design and synthesis of redox core–alpha amino acid composites based on thiol–disulfide exchange mechanism and a comparative study of their zinc abstraction potential from [CCXX] boxes in proteins

Subramania Ranganathan,[a,b,*] K. M. Muraleedharan,[a] Parimal Bharadwaj,[c] Dipankar Chatterji[d] and Isabella Karle[e,*]

[a]*Discovery Laboratory, Organic III, Indian Institute of Chemical Technology, Hyderabad 500 007, India*
[b]*Jawaharlal Nehru Centre for Advanced Scientific Research, Bangalore 560 012, India*
[c]*Department of Chemistry, Indian Institute of Technology, Kanpur 208 016, India*
[d]*Molecular Biophysics Unit, Indian Institute Science, Bangalore 560 012, India*
[e]*Laboratory for the Structure of Matter, Naval Research Laboratory, Washington, DC 20375-5341, USA*

Respectfully dedicated to Darshan Ranganathan who passed away on her 60th birthday (4 June 2001)

Received 2 October 2001; revised 7 January 2002; accepted 7 February 2002

Abstract—The design and synthesis of agents that can abstract zinc from their [CCXX] (C=cysteine; X=cysteine/histidine) boxes by thiol–disulfide exchange-having as control, the redox parities of the core sulfur ligands of the reagent and the enzyme, has been illustrated, and their efficiency demonstrated by monitoring the inhibition of the transcription of calf thymus DNA by *E. coli* RNA polymerase, which harbors two zinc atoms in their [CCXX] boxes of which one is exchangeable. Maximum inhibition possible with removal of the exchangeable zinc was seen with redox–sulfanilamide–glutamate composite. In sharp contrast, normal chelating agents (EDTA, phenanthroline) even in a thousand fold excess showed only marginal inhibition, thus supporting an exchange mechanism for the metal removal.

1. Introduction

The genesis of the present work pertains to recent reports on the fact that, in the maturation of HIV virus, a 55-residue protein called nucleocapsid protein (NCp7) plays a very important role in the proper packaging of HIV-RNA. Viral RNA, which provides all the information for its function, can be packaged only if this protein is present. The sequence of this protein is presented in Chart 1, **A**. The protein contains two zinc finger modules, where the metal is harbored in the [CCXX] boxes.[1] Concerted efforts to remove zinc from these efficiently, led to the identification of disulfides of the type **B** (Chart 1) as useful agents to disrupt the NCp7 conformation by the removal of the zinc present, thus making the protein inoperative and thereby making the packaging of virions in the HIV virus defective and dysfunctional.[2]

The efficiency with which zinc is removed from **A** by **B**, in the context of work from our laboratory,[3] provided an opportunity to design agents that could abstract zinc present in the [CCXX] boxes of enzymes, by the thiol–disulfide exchange mechanism (Chart 2).[4]

Thus, **B** (Chart 1) could react with an appropriate [CCXX] box harboring zinc in proteins, to form the octahedral complexes, which could break up, effecting oxidation in the [CCXX] box with concomitant removal of **B** as a zinc complex. The rationalization of the overall process in this manner brings to focus, the redox parity of the S–S system present in **A** and **B** (Chart 2).

The redox core in **B** was redesigned to interact favorably with the zinc finger modules, by linking with diverse amino acid residues. This was considered important, since, in the removal of zinc from [CCXX] boxes, the amino acid side chains could play a major role in stabilizing the transition state, by interaction with residues present in the zinc

Keywords: thiol–disulfide exchange; RNA polymerase; dithiobisbenzamides; benzisothiazolones.

* Corresponding authors. Address: Discovery Laboratory, Organic III, Indian Institute of Chemical Technology, Hyderabad 500 007, India. Tel.: +91-40-7160123x2648; fax: +91-40-7160757; e-mail: rangan@iict.ap.nic.in

0040–4020/02/$ - see front matter
PII: S0040-4020(02)00159-X

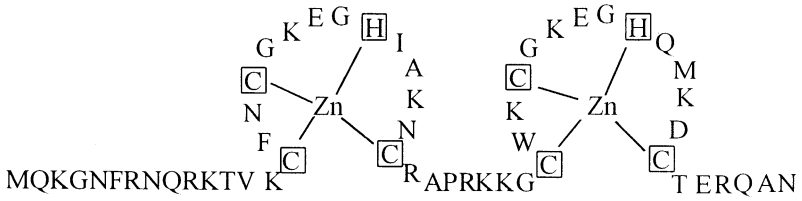

A

NCp7 sequence [G: Gly; A: Ala; V: Val; L: Leu; I: Ile; D: Asp; N: Asn; E: Glu; Q: Gln; K: Lys; R: Arg; H: His; S: Ser; T: Thr; F: Phe; Y: Tyr; W: Trp; C: Cys; M: Met; P: Pro.

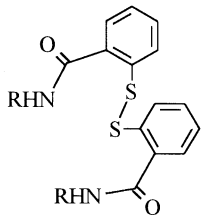

B

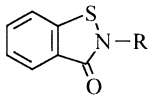

C

Chart 1.

protein/enzyme. In the zinc finger–DNA recognition, the importance of these interactions has been recognized.[5] The ease with which zinc complexes can be prepared from a [CCXX] box made it interesting to generate these, in an exchange process, leading to minimalistic zinc finger motifs by attachment of a histidine to the redox system in **B**. This approach has yielded good results.

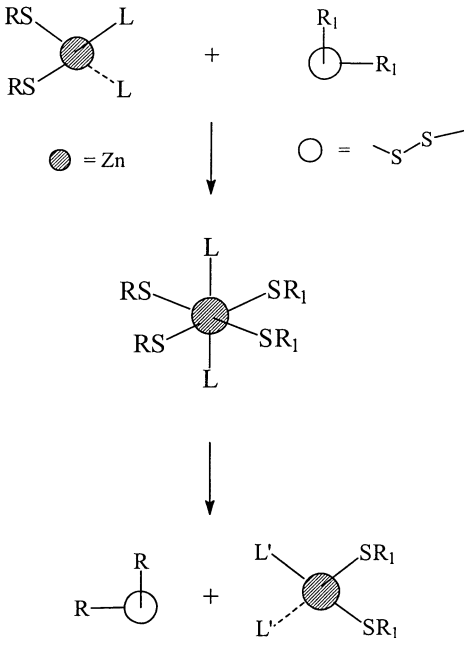

Chart 2.

2. Results and discussion

2.1. Synthesis and crystal structures

The reaction of 2,2′ dithiodibenzoyl chloride (**2**) with freshly prepared amino acid methyl esters of Ala, Aib, Val, Pro, Phe and Met, followed by column chromatography afforded the expected bisamides **3**–**8** (Chart 3).

Surprising results were obtained from amino acids that have a proton source in the side chain. They afforded benzisothiazolones (**9**, **11**, **13**–**15**: Chart 4) arising from cleavage of the S–S bond, with concomitant peptide NH participation. Tyrosine and threonine, in addition, gave the normal bisamides **10** and **12** (Chart 4).

In spite of sustained interest in redox systems of the type **B** (Chart 1), no crystal structure of this class of compound is available. Fortunately, the threonine linked bis amide **12** and the abnormal product **11** crystallized from $CHCl_3$/CH_3CN=1:1. The resulting X-ray structures are presented in Figs. 1 and 2.

The structure of **12** clearly showed the near orthogonal disposition of the two ligands of the disulfide unit and, as envisaged in Chart 2. Of additional interest is the generalized hydrogen bonding seen, involving the amide unit,

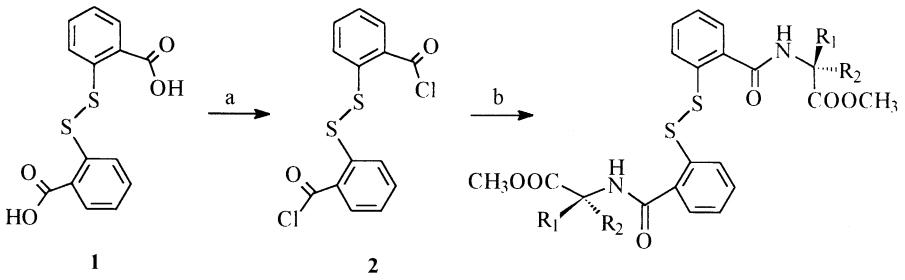

a) $SOCl_2$, reflux b) H_2N-(AA)-$COOCH_3$, Et_3N, CH_2Cl_2

	R_1	R_2	AA	(%)
(3)	CH_3	H	Ala	25
(4)	CH_3	CH_3	Aib	24
(5)	$(CH_3)_2CH$	H	Val	63
(6)	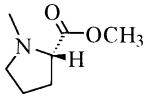		Pro	43
(7)	CH_2Ph	H	Phe	36
(8)	$CH_3SCH_2CH_2$	H	Met	75

Chart 3.

which is augmented by the hydrogen bonding with the threonine hydroxyl group. These interactions are likely to hold the disulfide group exposed, thus making its approach to the enzyme metal center facile (Chart 2).

The X-ray structure of the benzisothiazolone **11** (Fig. 2) showed no surprises. This class of compounds is stable and therefore these molecules are potentially better drug candidates, compared to the dimeric bisamides.

The benzisothiazolone **9** from tyrosine gave crystals from $CHCl_3/CH_3CN$=1:1. The X-ray structure presented in Fig. 3 shows an orthogonal disposition of the tyrosine aromatic residue. Here also the S–N bond involved in the thiol–disulfide exchange is exposed.

The bisamides and benzisothiazolones can be spectroscopically distinguished. In their FAB mass spectra, the bisamides display protonated mass peaks and those complexed with sodium ions. They invariably show base peaks corresponding to the clean rupture of the S–S bonds. The fact that these were actually generated in the mass spectrometer was evidenced by the fact that, they appeared uncomplexed with the proton, as is always the case with parent ions. In sharp contrast, the benzisothiazolones gave peaks corresponding to the mass with a proton.

A characteristic feature that distinguishes the bisamides from the benzisothiazolones is the appearance of the Cα proton at, respectively, ~4.5 and ~5.5 ppm in the NMR spectrum. The isolation of the benzisothiazolones is significant in the sense that, although the formation of such compounds has been speculated in the fragmentation of bisamides (Chart 1, **C**), they have never been isolated pure and adequately characterized.

Hitherto, the bisamide→benzisothiazolone change was rationalized on the basis of a nucleophilic attack by the amide nitrogen on the dithio bond, resulting in S–S cleavage to benzisothiazolone on the one hand and the corresponding –SH compound on the other. This mechanism would envisage loss of 50% of the starting compound. The fact that, in the case of threonine, not only the benzisothiazolone (**11**) was secured in 59%, but also, the bisamide (**12**) was isolated in 31% yield, would require a revision of this mechanism. We propose that, in the cases where there is a proton source available in the side chain, the protonated intermediate undergoes rupture to give the benzisothiazolone on the one hand and the –SH species on the other. The process operates in a cyclic form by the transformation of the latter by oxidation, to the bisamide. This pathway would account for as much as 100% yields of benzisothiazolones (Chart 5). The facile oxidation of the intermediate SH compounds to the bisamides has been experimentally verified.

The consequences of two alterations—the introduction of spacer between the redox core and the amino acid, and the tethering of the termini—that could have a bearing on the proclivity for exchange, were examined.

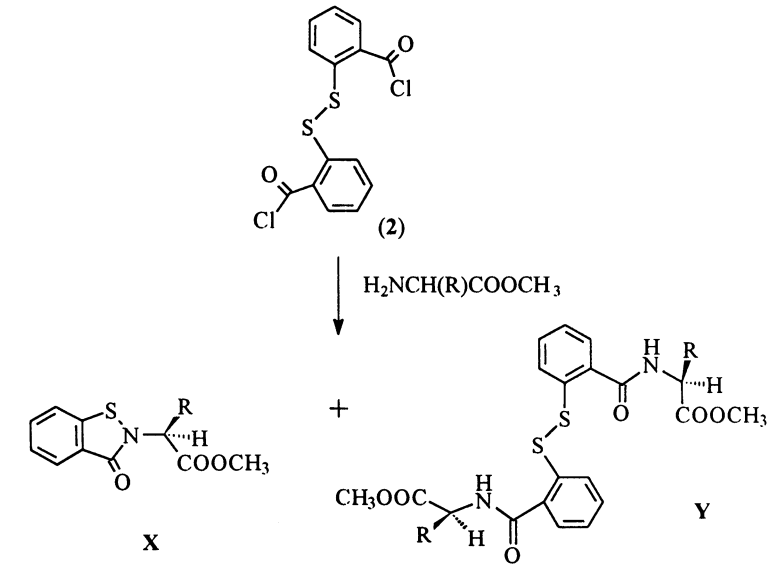

R	AA	X (%)	Y (%)
$-CH_2-C_6H_4-OH$	(Tyr)	**9** (29)	**10** (19)
$-CH(CH_3)OH$	(Thr)	**11** (59)	**12** (31)
$-CH_2OH$	(Ser)	**13** (41)	–
$-CH_2-C_8H_6N$	(Trp)	**14** (25)	–
$-CH_2-C_3H_3N_2$	(His)	**15** (56)	–

Chart 4.

The sulfanilamide–redox composite (**16**), prepared from **2** and sulfanilamide, on coupling with Boc-Glu(γOMe)OH afforded the redox–spacer–aminoacid composite **17** (Chart 6). This coupling is noteworthy since amidation involving a charge depleted SO_2NH_2 unit is rare.

The reaction of **2** with freshly prepared cystine-di-OMe afforded three compounds, namely, the desired tethered system **20** and fragmentation products **18** and **19** (Chart 7). Compound **19** crystallized from EtOAc/hexane=1:1. The crystal structure of **19** (Fig. 4) consists of, in the unit cell, a heterodimer arising from strong hydrogen bonding of the nearly *cis* oriented amides to form an 8-ring non-covalent assembly. Such dimer formation was also seen in the mass spectrum of **19**, which showed a significant peak at 475 $(2M+H)^+$. Compounds of type **19** are potent angiotensin II inhibitors in their own right.[6] Compounds **18** and **19** arise from fragmentation of the composite **20**. Methanolic solutions of pure **20**, admixed with triethylamine, rapidly generated the fragmentation products. It is suggested that, arising from steric constraints imposed on the system by tethering, fragmentation occurs via formation of a dehydro Ala on the one hand and an S–S cleavage on the other, and this by processes, similar to that for benzisothiazolone formation (Chart 5), is transformed in to **18** and **19** (Chart 8).

The reaction of **2** with *o*-phenylenediamine afforded the benzisothiazolone **21**, the symmetrical monocyclic 2+2 adduct **22** and none of the 1:1 tethered system (Chart 9).

Compound **21** crystallized from EtOAc/hexane=1:1. The crystal structure is presented in Fig. 5. Unlike the other examples (**9** and **11**), the molecule **21** is nearly planar with proximal alignment of the amino group to the sulfur atom, rather than to the carbonyl of the benzisothiazolone. The mass spectrum of **22** exhibited a peak at 756 $(M+H)^+$. This compound is interesting in that, within the confines of a Ar–S–S–Ar periphery, the cavity is highly programmed for the uptake of ions, possessing as it does, four rigidly aligned peptide groups.

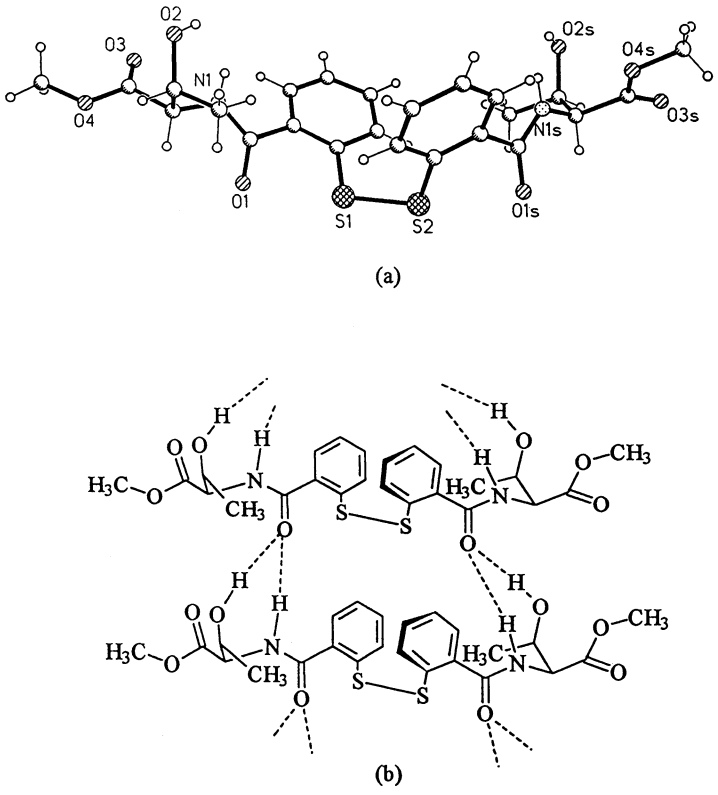

Figure 1. (a) Crystal structure of **12**. (b) Extended hydrogen-bonded assembly of **12** in the crystal lattice. The distances in the hydrogen bonds (dashed lines) are O2–O1=2.895 Å, N1–O1=2.949 Å. O2s–O1s=3.102 Å, N1s–O1s=2.908 Å.

2.2. Preliminary assessment of the design

Evidence for the operation of the two main features of the design, namely, zinc abstraction by thiol–disulfide exchange and the importance of the amino acid ligand present in the composite were sought by monitoring the course of transcription of calf thymus DNA by *E. coli* RNA polymerase[7] after treatment with either the dithiobisbenzamides (**3**–**8**, **10**, **12**, **16**, **17** and **20**) or benzisothiazolones (**11**, **14**, and **15**).[8] The latter class has not been envisaged for use in metal abstraction.

The results are presented in a graphical format in Fig. 6. For comparison purposes, the enzyme activity without the reagent was taken as 100% and the outcome from other experiments are made based on this standard. To enable a direct comparison, the results from normal chelating agents like EDTA and *o*-phenanthroline at much higher concentrations ($\sim\times10^4$) are also presented in Fig. 6, which also incorporates results from use of a 10-fold excess of selected reagents. At higher concentrations ($\sim\times10^4$), all the reagents totally inhibited transcription.

The effect of zinc removal from yeast RNA polymerase II on transcription profile has been studied.[9] Of the two zinc atoms present in the enzyme, one could be removed rather

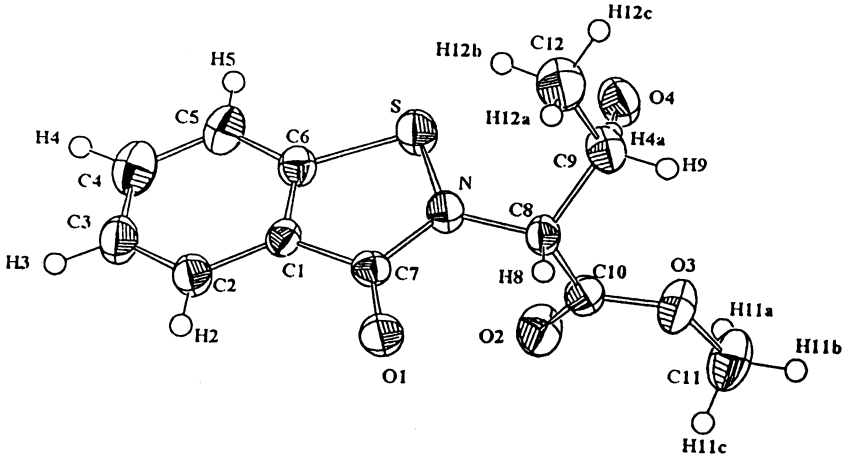

Figure 2. Crystal structure of **11**.

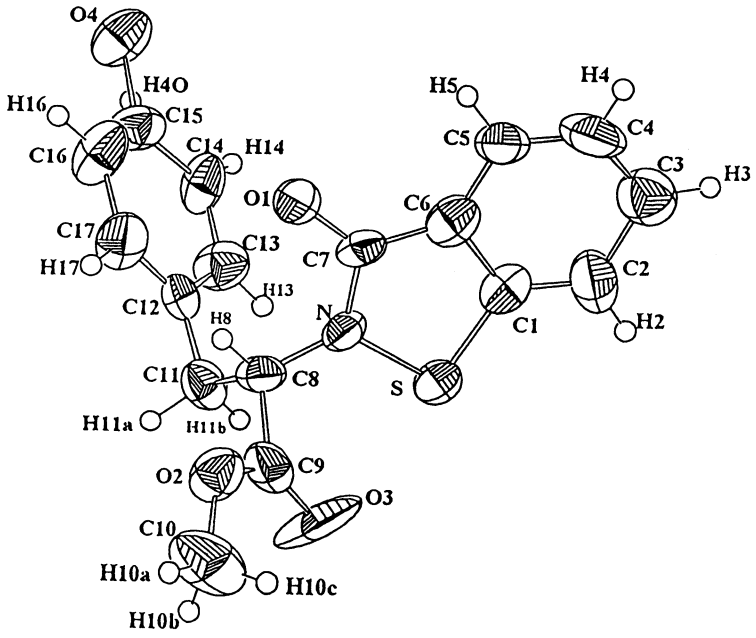

Figure 3. Crystal structure of **9**.

easily, leading to a mono zinc depleted modified enzyme which still showed ~35% of original activity. The removal of both zinc atoms requires rather drastic conditions and the resulting totally zinc depleted enzyme does not show any transcription activity. Recent studies with *E. coli* RNA polymerase[10] has led to remarkably similar conclusions. The 1407 residue β′ fragment harbor in their [CCXX] boxes, the two zinc atoms. Whilst the zinc is bound tightly in the N-terminal location, and could not be exchanged readily, that present at the C-terminal can be exchanged and reconstituted with only partial loss of activity. Present studies with *E. coli* RNA polymerase has clearly shown that, with excess of the reagent, both zinc ions are removed, resulting in the total inhibition of transcription and with two equivalents of the reagent, only one zinc is removed, resulting in the retention of a third of the activity of the native enzyme.

With an equivalent of the reagent for each zinc ion, the inhibition varied from 1% for Pro-bisamide (**6**) to 62% for the core–sulfanilamide–Glu composite **17**. The 62% inhibition by **17** represents the removal of one zinc from the enzyme. This threshold was reached by the Ala-bisamide (**3**) and the Met-bisamide (**8**) at a 10-fold increased concentration.

A striking observation from Fig. 6 is that the reagents studied here are far superior in the removal of metal, compared to the traditional chelators like EDTA and *o*-phenanthroline. Even at enhanced concentrations [EDTA: ×12,500; *o*-phenanthroline: ×6250], they were not able to effect significant removal of the metal, which provides strong support for the thiol–disulfide exchange mechanism envisaged here (Chart 2) and rules out a simple chelation path. This understanding will be helpful in the

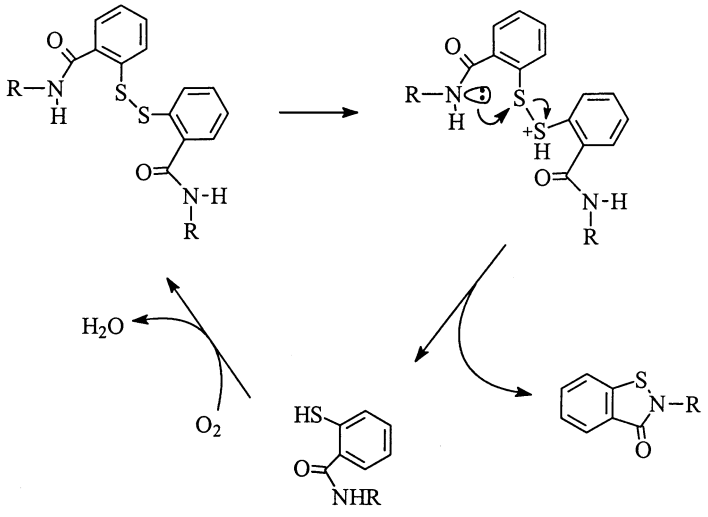

Chart 5.

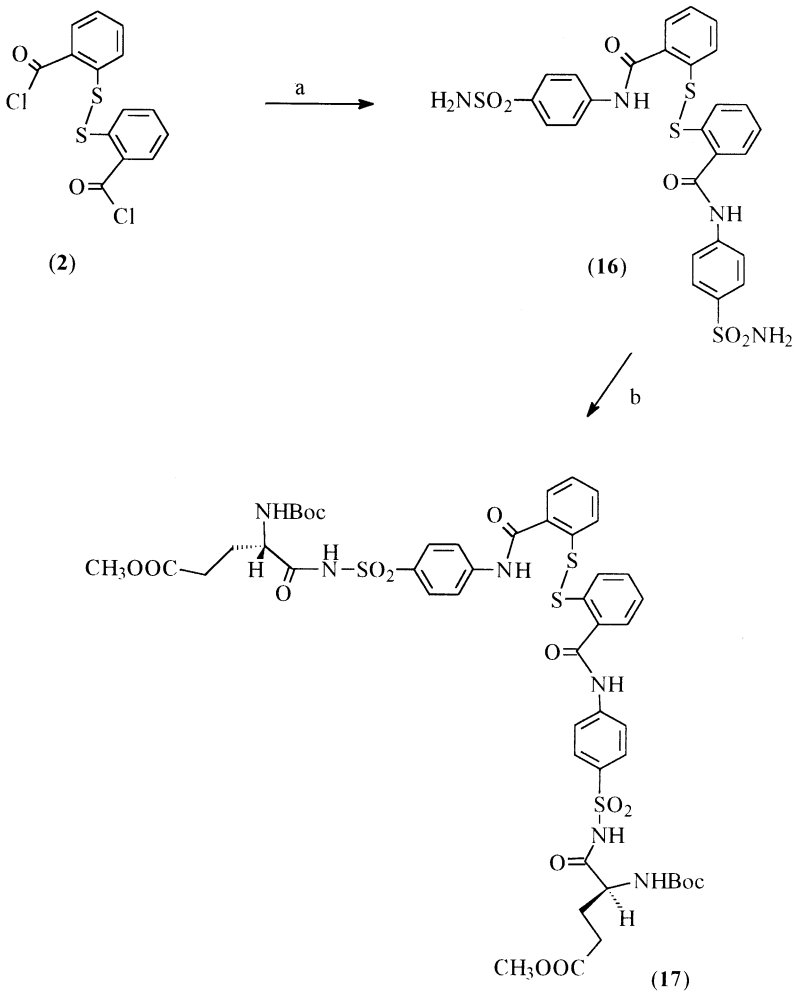

a) Sulfanilamide, Py. b) BocGlu(γOMe)OH, DCC, DMF.

Chart 6.

further development of proper reagents for the abstraction of zinc.

Fig. 6 neatly divides the reagents studied in this work into two categories. Those which are on the left side of *o*-phenanthroline and EDTA (at vastly enhanced concentrations) and the others to the right of it. The former constitute a class having decreased capacity for inhibition of transcription process by *E. coli* RNA polymerase and the latter, a vastly enhanced inhibitory profile. It cannot be a coincidence that a better profile is shown by hydrophobic amino acid derivatives (Phe, Val, Ala, Aib, Tyr). This preference profile strongly supports the notion that amino acids attached to the redox core can play a role in the stabilization of the transition state involved in the exchange (Chart 2).

The fact that hydrophobic amino acids are able to promote such stabilization indicates the importance of such interactions in the vicinity of the [CCXX] box in *E. coli* RNA polymerase. Of the 30 residue C-terminal segment of the β′ subunit of *E. coli* RNA polymerase, that harbor the exchangeable zinc in a [CCCH] box[10] (Chart 10), as many as 12 are hydrophobic (others: Gly, 3; polar, 4; acidic, 3; basic, 4 and CCCH box).

The importance of amino acid attachment in the design is again highlighted with the pairs **16** and **17**. Compound **16** exhibited the maximum potential in the removal of zinc from NCp7. However, with RNA polymerase, the activity is modest. This profile is greatly enhanced from 31 to 62% inhibition by simple attachment of the glutamate residue.

The near complete lack of activity of the proline bisamide **6** clearly brings out the important role of the peptide NH in the exchange process. Contrary to expectations, the cystine-di-OMe tethered composite **20** exhibited poor activity (13%), compared to the structurally closest open compound from Ala (**3**) (47%). Minimum energy conformations of the cyclic compound **20** and the open **3** derived using simulated annealing molecular dynamics (MD)

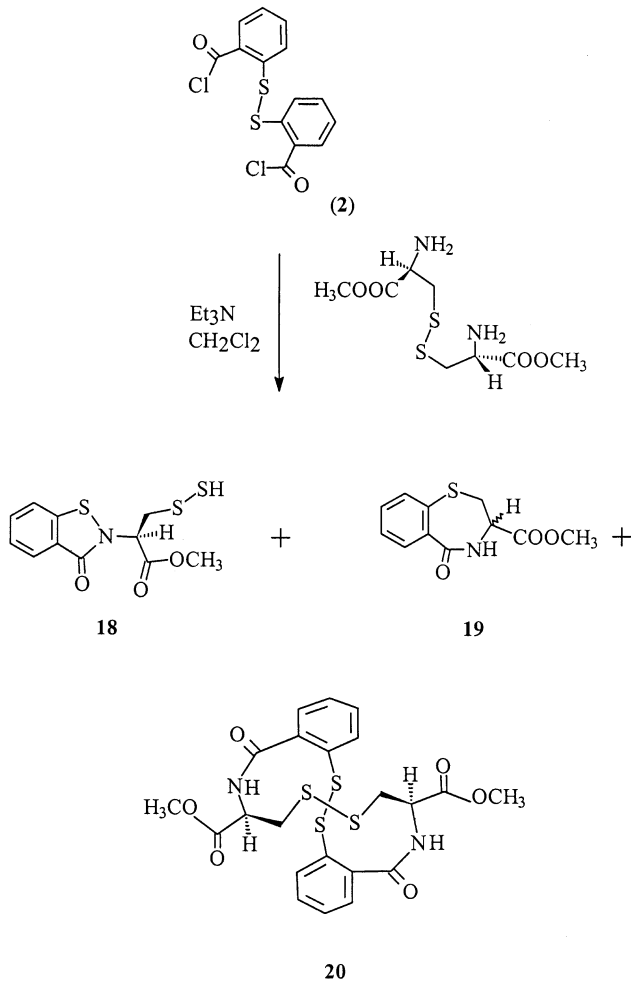

Chart 7.

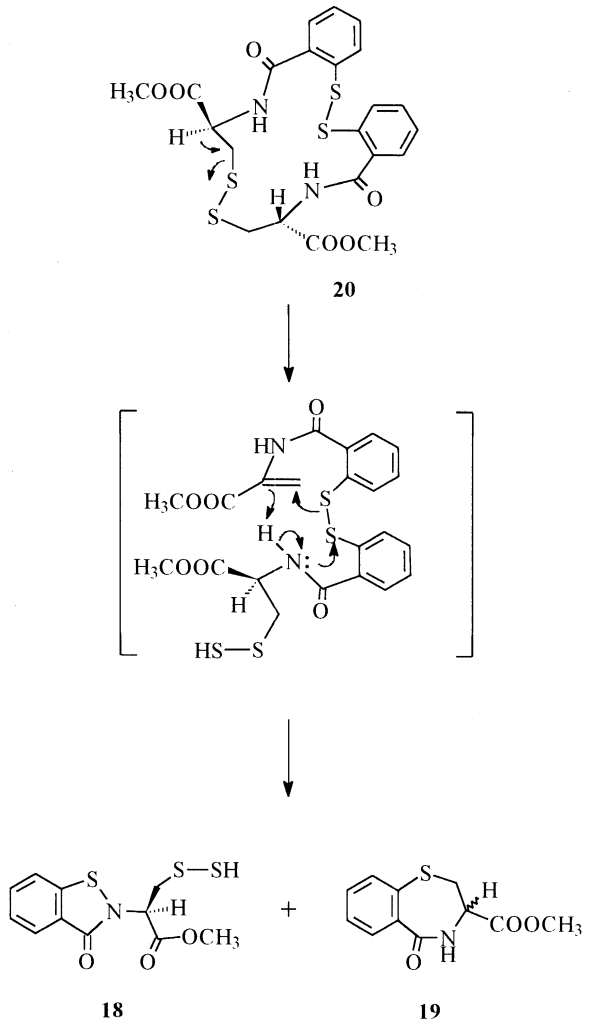

Chart 8.

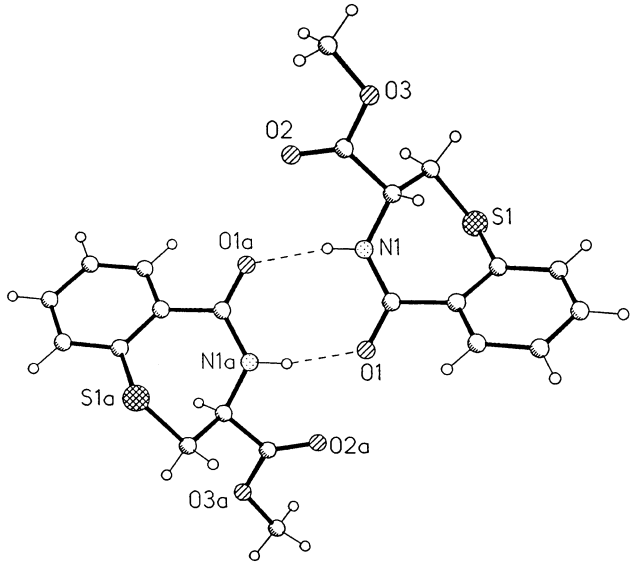

Figure 4. Crystal structure of **19** as hydrogen bonded dimer. The two N–O═C distances (dashed lines) are 2.895 and 2.910 Å.

suggest that approach to the redox active aromatic disulfide core is greatly hindered in the case of the cyclic compound **20**.[11]

A novel finding of the present work is the clear establishment of the ability of benzisothiazolones to abstract zinc, most likely involving the S–N bond in the exchange (Chart 11). Interestingly, such an exchange with the imidazole containing isothiazolone **15** would result in complex, reminiscent of a minimalistic zinc finger motif[3] (Chart 12). The observed exceptional activity of **15** could arise from this combination of properties. In view of the known biological profile of isothiazolones, this property suggests further avenues for exploration.

On the basis of observations presented here, it is suggested that the removal of zinc present in [CCXX] boxes of proteins/enzymes takes place by a thiol–disulfide exchange mechanism (Chart 2). Thiol–disulfide exchange is an important process in biological systems,[4] the ramifications of which are being increasingly understood and exploited. The most attractive feature of this process is that the metal transfer takes place on a common template, leading to clean reactions, avoiding leakage of open ligands.

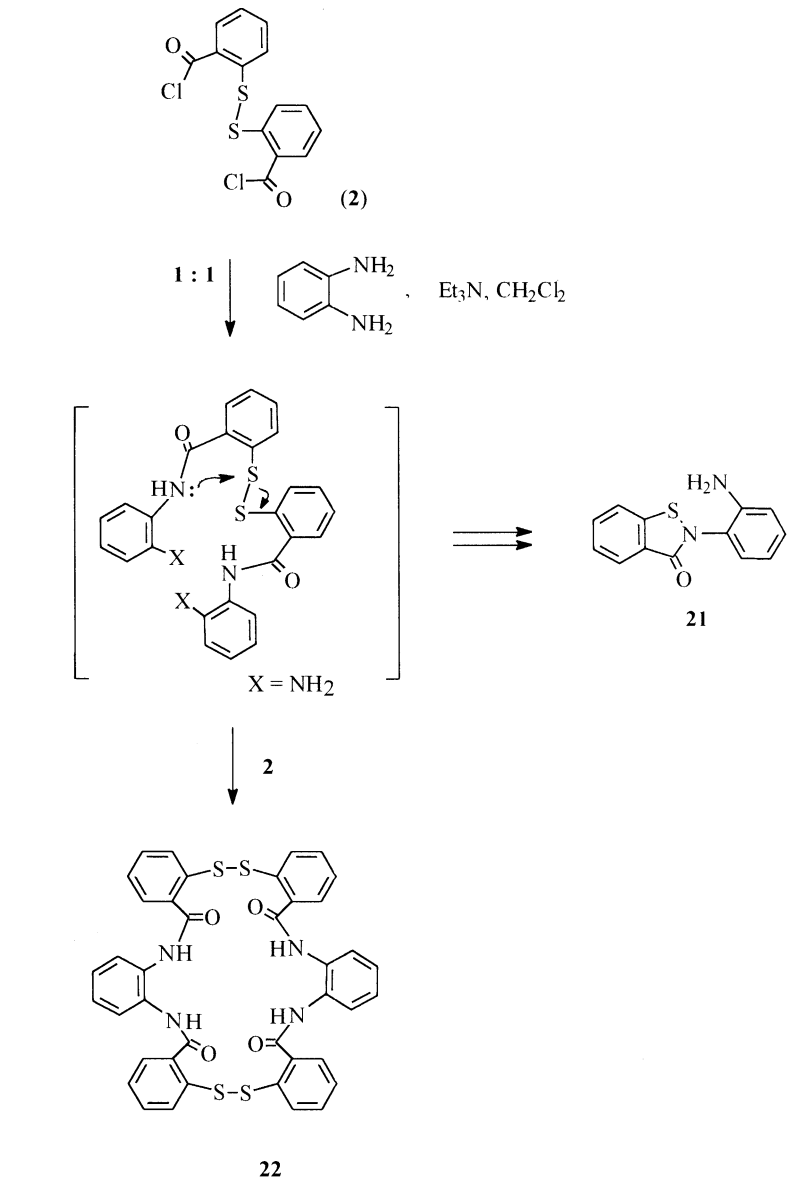

Chart 9.

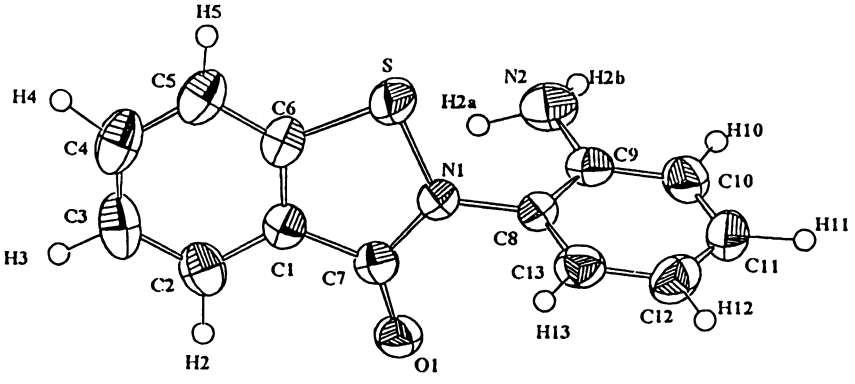

Figure 5. Crystal structure of **21**.

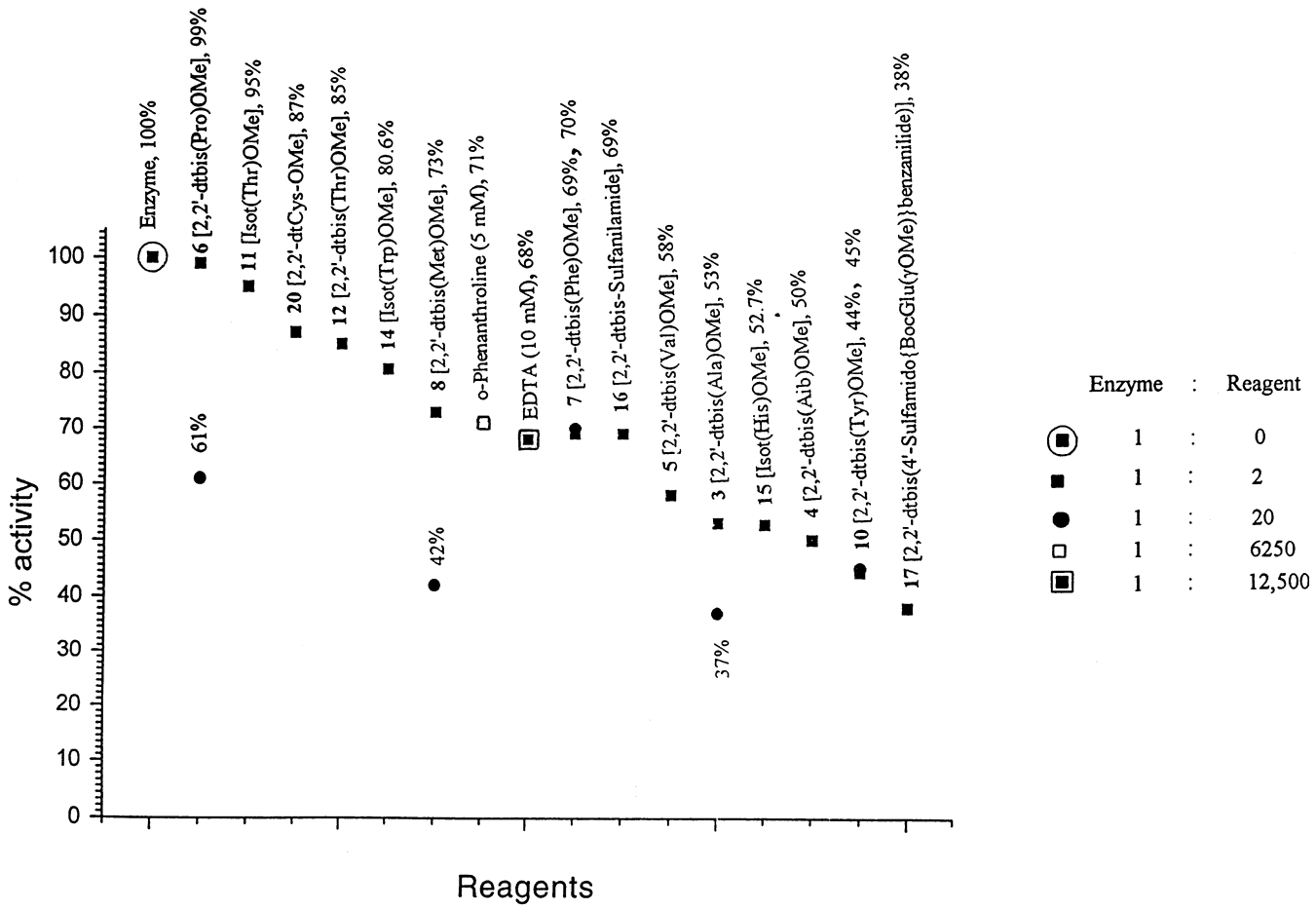

Figure 6. *E. Coli* RNA polymerase inhibition with dithiobisbenzamides [2,2′-dtbis(AA)OMe] and benzisothiazolones [Isot(AA)OMe] (AA=amino acid).

3. Experimental

3.1. Materials and methods

All amino acids used were of L-configuration. Melting points were recorded on a Fisher–Johns melting point apparatus and are uncorrected. Optical rotations were measured with an automatic JASCO polarimeter; concentrations are given in grams/100 mL. Infra red spectra were recorded on a Perkin–Elmer/1600-FT spectrometer either as neat liquids or as KBr pellets and prominent peaks are expressed in cm^{-1}. ^{1}H and ^{13}C NMR spectra were recorded on Bruker WM-300 NMR spectrometer. The chemical shifts are expressed in δ (ppm) with TMS at 0.000 as the internal reference. FAB MS were obtained on a JEOL SX-120/DA-6000 instrument using *m*-nitrobenzylalcohol as the matrix. C, H, N analysis was carried out in Vario EL elemental

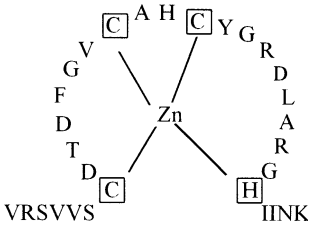

Chart 10.

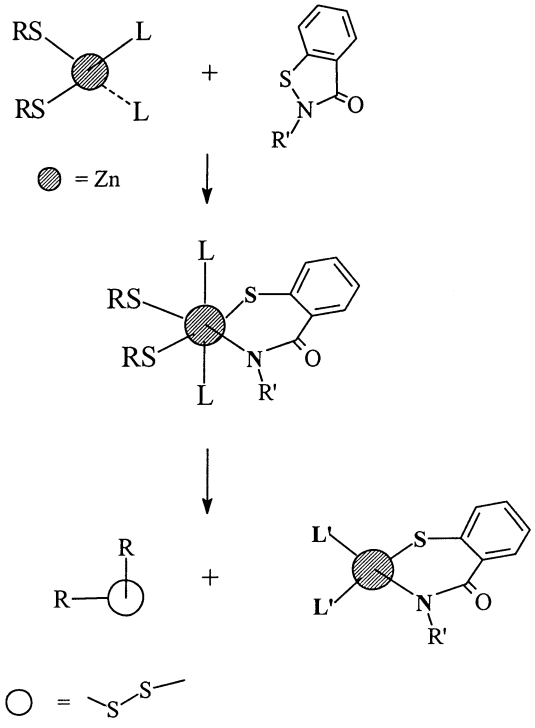

Chart 11.

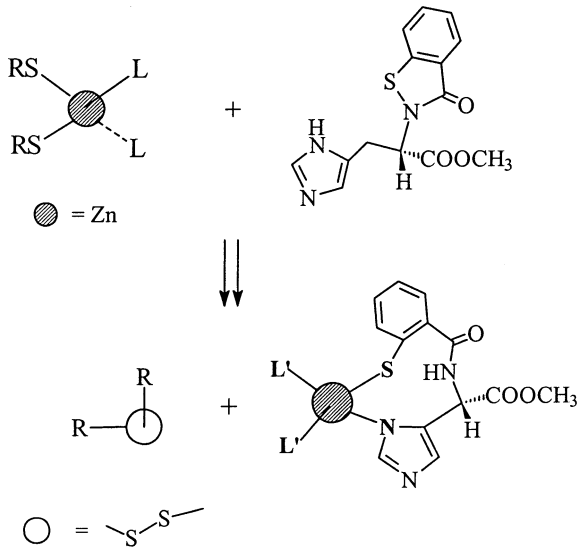

Chart 12.

analyzer. Reactions were monitored wherever possible by TLC (silica gel/G (Merck) and the eluent (invariably ethyl acetate/hexane) ratio adjusted to give Rf values in the range of 0.4–0.6. Column chromatography was done on silica gel (100–200 mesh) columns, which were generally made from a slurry in hexane or a mixture of hexane and ethyl acetate. Products were eluted with a mixture of ethyl acetate/hexane.

3.2. Synthesis

3.2.1. 2,2′-Dithiodibenzoyl chloride (2). A mixture of 2,2′-dithiodibenzoic acid (**1**) (2 g, 6.53 mmol) and $SOCl_2$ (24 mL) was refluxed for 24 h, evaporated, the residue dissolved in CH_2Cl_2 (5 mL), evaporated in vacuo, triturated with dry hexane, filtered under protection from moisture, washed with dry hexane and dried over P_2O_5 to afford 1.5 g (67%) of **2** (waxy solid).

Mp: 148°C (Lit.[2a] mp 150–152°C); IR (KBr): 1721, 1600, 1560; ^{1}H NMR ($CDCl_3$–DMSO-d_6) δ 7.4 (dd, J=13.8, 0.5 Hz, 2H), 7.6 (dd, J=13.8, 0.5 Hz, 2H), 7.7 (dd, J=10, 0.5 Hz, 2H), 8.08 (dd, J=10, 0.5 Hz, 2H) (aromatic).

3.3. The reaction of 2,2′-dithio dibenzoylchloride with α aminoacid methyl esters: isolation of 2,2′-dithiodibenzoyl bis-aminoacid methyl esters (3–8, 10 and 12) and *N*-(benzisothiazolone) amino acid methyl esters (9, 11 and 13–15) (general procedure)

A solution of 2,2′-dithiodibenzoyl chloride (**2**) (1 g, 2.915 mmol) in dry CH_2Cl_2 (25 mL) and 0.9 mL (6.413 mmol) of triethylamine were simultaneously added dropwise to an ice cooled and stirred solution of the free amine of the amino acid methyl ester (generated in situ by the addition of triethylamine (6.413 mmol) to an ice cooled and stirred suspension of the amino acid methyl ester hydrochloride (6.413 mmol) in dry CH_2Cl_2 (60 mL). (In the case of histidine methyl ester dihydrochloride, 12.8 mmol of triethylamine was used.) The reaction was stirred for 48 h at room temperature, washed successively with cold saturated $NaHCO_3$ (3×10 mL), 1 M H_2SO_4 (3×10 mL) and then with distilled water (1×10 mL) (in the case of Trp and His, the acid wash was not done). The organic layer was dried ($MgSO_4$), evaporated in vacuo and the residue chromatographed on a silica gel using hexane–EtOAc as eluent. When present, the benzisothiazolones eluted earlier than 2,2′-dithiobisbenzamides. Characteristic spectral features of the products (**3**–**15**) obtained on using various amino acids (AA) are presented below.

3.3.1. Compound 3. Dithiobisbenzamide: AA=Ala; white powder; yield: 25%; $[\alpha]_D^{29}=-10.00$ (c 1, $CHCl_3$); mp 104–106°C; IR (KBr): 3306, 3012, 1749, 1651, 1545; ^{1}H NMR ($CDCl_3$) δ 1.56 (d, J=7 Hz, 6H, CH_3), 3.8 (s, 6H, $COOCH_3$), 4.7–4.8 (m, 2H, $C^{\alpha}H$), 6.78 (d, J=3 Hz, 2H, NH), 7.2–7.77 (m, 8H, ArH); FAB MS (*m*/*z*) (%): 477 (10) $(MH)^+$, 499 (5) $(M+Na)^+$, 238 (100) (M/2); Anal. Found: C, 55.01; H, 5.38; N, 5.80. Calcd for $C_{22}H_{24}N_2O_6S_2$: C, 55.46; H, 5.04; N, 5.88.

3.3.2. Compound 4. Dithiobisbenzamide: AA=Aib; white powder; yield: (24%); mp 178–180°C; IR (KBr): 3245, 2989, 1748, 1634, 1539; ^{1}H NMR ($CDCl_3$) δ 1.69 (s, 12H, CH_3), 3.79 (s, 6H, $COOCH_3$), 6.76 (brs, 2H, NH), 7.2–7.76 (m, 8H, ArH); FAB MS (*m*/*z*) (%): 527 (7) $(M+Na)^+$, 252 (100) (M/2); Anal. Found: C, 57.55; H, 5.34; N, 4.80. Calcd for $C_{24}H_{28}N_2O_6S_2$: C, 57.14; H, 5.55; N, 5.55.

3.3.3. Compound 5. Dithiobisbenzamide: AA=Val; white powder; yield: 63%; mp 148–150°C; $[\alpha]_D^{29}=-3.00$ (c 1, $CHCl_3$); IR (KBr): 3293, 2963, 1744, 1634, 1529; ^{1}H NMR ($CDCl_3$) δ 0.98 (d, J=7 Hz, 6H), 1.0 (d, J=7 Hz, 6H), 2.3 (m, 2H, $C^{\beta}H$), 3.79 (s, 6H, $COOCH_3$) 4.81 (m, 2H, $C^{\alpha}H$), 6.63 (d, J=3 Hz, 2H, NH), 7.2 (dd, J=8, 0.5 Hz, 2H), 7.3 (dd, J=8, 0.52 Hz, 2H), 7.6 (d, J=8 Hz, 2H), 7.75 (d, J=8 Hz, 2H) (aromatic); FAB MS (*m*/*z*) (%): 533 (44) $(MH)^+$, 555 (10) $(M+Na)^+$, 266 (100) (M/2); Anal. Found: C, 58.58; H, 6.01; N, 5.03. Calcd for $C_{26}H_{32}N_2O_6S_2$: C, 58.64; H, 6.01; N, 5.26.

3.3.4. Compound 6. Dithiobisbenzamide: AA=Pro; pale yellow solid; yield: 43%; IR (neat): 2961, 1752, 1652, 1631, 1415; ^{1}H NMR ($CDCl_3$) δ 1.88–2.32 (m, 8H, C^{β} and $C^{\gamma}H_2$), 3.3–3.44 (m, 4H, $C^{\delta}H_2$), 3.79 (s, 6H, $COOCH_3$), 4.69 (m, 2H, $C^{\alpha}H$), 7.18–7.33 and 7.71–7.74 (m,m, 8H, ArH); FAB MS (*m*/*z*) (%): 529 (59) $(MH)^+$, 551 (13) $(M+Na)^+$, 264 (100) (M/2); Anal. Found: C, 59.51; H, 5.54; N, 4.92. Calcd for $C_{26}H_{28}N_2O_6S_2$: C, 59.09; H, 5.30; N, 5.30.

3.3.5. Compound 7. Dithiobisbenzamide: AA=Phe; yellow powder; yield: (36%); mp 174–176°C; $[\alpha]_D^{29}=+112.00$ (c 1, $CHCl_3$); IR (KBr): 3285, 3036, 1742, 1640, 1533; ^{1}H NMR ($CDCl_3$) δ 3.3 (dq, J=14, 3 Hz, 4H, $C^{\beta}H_2$), 3.78 (s, 6H, $COOCH_3$), 5.1 (m, 2H, C^{α}Hs), 6.57 (d, 2H, NHs), 7.15–7.74 (m, 16H, Phe ArHs+dithio ArHs), 7.75 (d, 2H, dithioArHs); FAB MS (*m*/*z*) (%): 629 (30) $(MH)^+$, 651 (7) $(M+Na)^+$, 314 (100) (M/2); Anal. Found: C, 65.03; H, 5.05; N, 4.20. Calcd for $C_{34}H_{32}N_2O_6S_2$: C, 64.96; H, 5.09; N, 4.45.

3.3.6. Compound 8. Dithiobisbenzamide: AA=Met; yellow powder; yield: (75%); mp 206–208°C; $[\alpha]_D^{29}=+8.00$ (c 1, $CHCl_3$); IR (KBr): 3265, 3070, 1755, 1640,

1546; ^{1}H NMR ($CDCl_3$) δ 2.10 (s, 6H, $-SCH_3$), 2.1–2.33 (m, 4H, $C^{\beta}H_2$), 2.63 (m, 4H, $C^{\gamma}H_2$), 3.81 (s, 6H, $COOCH_3$), 4.94 (m, 2H, $C^{\alpha}H$), 6.93 (d, J=3 Hz, NH), 7.25 (dd, J=8, 0.5 Hz, 2H), 7.4 (dd, J=10, 0.5 Hz, 2H) 7.6 (d, J=8 Hz, 2H), 7.8 (d, J=8 Hz, 2H) (ArH); FAB MS (m/z) (%): 597 (48) $(MH)^+$, 619 (11%) $(M+Na)^+$, 298 (100) (M/2); Anal. Found: C, 51.90; H, 5.30; N, 4.28. Calcd for $C_{26}H_{32}N_2O_6S_2$: C, 52.34; H, 5.37; N, 4.70.

3.3.7. Compound 9. Benzisothiazolone: AA=Tyr; pale yellow needles; yield: (29%); mp 188–190°C; $[\alpha]_D^{29}$= −63.00 (c 1, $CHCl_3$); IR (KBr): 3421 (br), 3161, 1752, 1636, 1599, 1518, 1449; ^{1}H NMR ($CDCl_3$) δ 3.15 (dd, J=10, 4 Hz, 1H), 3.5 (dd, J=10, 2 Hz, 1H, $C^{\beta}H_2$) 3.76 (s, 3H, $COOCH_3$), 5.75 (m, 1H, $C^{\alpha}H$), 6.7 (d, J=8 Hz, 2H), 7.0 (d, J=8 Hz, 2H) (, Tyr), 7.29, 7.54, 7.94 (m,m,m, 4H, ArH); ^{13}C NMR ($CDCl_3$) δ 36.78 (C^{β}), 52.79 (C^{α}), 57.03 ($-OCH_3$), 115.66–155.66 (C aromatic), 166.24 (–COO–), 170.25 (Ar-CO); FAB MS (m/z) (%): 330 (100) $(MH)^+$, 352 (7) $(M+Na)^+$ 659 (6) $(2M+H)^+$; Anal. Found: C, 61.89; H, 4.64; N, 3.98. Calcd for $C_{17}H_{15}NO_4S$: C, 62.00; H, 4.56; N, 4.26.

3.3.8. Compound 10. Dithiobisbenzamide: AA=Tyr; white solid; yield: (19%); Anal. Found: C, 61.52; H, 5.01; N, 4.71; mp 229–231°C; Calcd For $C_{34}H_{32}N_2O_8S_2$: C, 61.81; H, 4.84; N, 4.24; $[\alpha]_D^{29}$=+28.00 (c 0.5, $CHCl_3$); IR (KBr): 3366 (br), 3279, 3022, 1735, 1640, 1512, 1438; ^{1}H NMR ($CDCl_3$–DMSO-d_6) δ 3.14 (m, 4H, $C^{\beta}H_2$), 3.74 (s, 6H, $COOCH_3$), 4.8 (m, 2H, $C^{\alpha}H$), 6.7 (d, J=8 Hz, 4H), 7.1 (d, J=8 Hz, 4H) (Tyr H), 7.2, 7.4, 7.6, 7.8 (m,m,m,m, 8H, ArH), 8.01 (br, 2H, NH), 8.89 (s, 2H, OH); ^{13}C NMR ($CDCl_3$) δ 35.56 (C^{β}), 51.38 (C^{α}), 53.55 ($-OCH_3$), 114.67–155.35 (C aromatic), 166.70 (–COO–), 171.36 (Ar-CO); FAB MS (m/z) (%): 661 (49) $(MH)^+$, 683 (10) $(M+Na)^+$, 330 (100) (M/2); Anal. Found: C, 61.78; H, 5.21; N, 4.18. Calcd for $C_{34}H_{32}N_2O_8S_2$: C, 61.82; H, 4.85; N, 4.24.

3.3.9. Compound 11. Benzisothiazolone: AA=Thr; white solid; yield: (59%); mp 144–146°C; $[\alpha]_D^{29}$=−80.00 (c 0.5, $CHCl_3$); IR (KBr): 3496 (br), 2992, 1732, 1670, 1450; ^{1}H NMR ($CDCl_3$) δ 1.25 (d, J=7 Hz, 3H, CH_3), 3.1 (m, 1H, OH), 3.77 (s, 3H, $COOCH_3$), 4.72 (m, 1H, $C^{\beta}H$), 5.41 (m, 1H, $C^{\alpha}H$), 7.4 (dd, J=8, 0.5 Hz, 1H), 7.6 (d, J=8 Hz, 1H), 7.7 (d, J=8 Hz, 1H), 8.1 (d, J=8 Hz, 1H) (ArH); ^{13}C NMR ($CDCl_3$) δ 19.21 (C^{γ}), 52.86 (C^{β}), 60.95 (C^{α}), 67.38 ($-OCH_3$), 120.1–142.1 (C aromatic), 166.8 (–COO), 169.42 (Ar-CO); FAB MS (m/z) (%): 268 (100) $(MH)^+$, 290 (21) $(M+Na)^+$ 535 (3) $(2M+H)^+$, 557 (2) $(2M+Na)^+$; Anal. Found: C, 54.08; H, 4.86; N, 5.01. Calcd for $C_{12}H_{13}NO_4S$: C, 53.93; H, 4.86; N, 5.24.

3.3.10. Compound 12. Dithiobisbenzamide: AA=Thr; white solid; yield: (31%); mp 182–184°C; $[\alpha]_D^{29}$=−40.00 (c 0.5, $CHCl_3$); IR (KBr): 3527 (br), 3331, 2980, 1751, 1633, 1541, 1439, 1259; ^{1}H NMR ($CDCl_3$) δ 1.31 (d, J=6 Hz, CH_3), 2.86 (br, 2H, –OH), 3.79 (s, 6H, $COOCH_3$), 4.4 (br, 2H, NH), 4.7 (d, J=4 Hz, 2H, $C^{\beta}H$), 4.8 (d, J=4 Hz, 2H, $C^{\alpha}H$), 7.25, 7.4, 7.75, 7.85 (m,m,m,m, 8H, ArH); ^{13}C NMR ($CDCl_3$) δ 19.81 (C^{γ}), 51.78 (C^{β}), 57.99 (C^{α}), 66.99 ($-OCH_3$), 125.29–137.15 (C aromatic), 167.5 (–COO), 170.71 (Ar-CO); FAB MS (m/z) (%): 537 (12) $(MH)^+$, 559 (12) $(M+Na)^+$, 268 (100) (M/2); Anal. Found: C, 53.61; H, 5.20; N, 4.98. Calcd for $C_{24}H_{28}N_2O_8S_2$: C, 53.73; H, 5.22; N, 5.22.

3.3.11. Compound 13. Benzisothiazolone: AA=Ser; white powder; yield: (41%); mp 153–155°C; Anal. Found: C, 51.74; H, 5.41; N, 5.56; Calcd For $C_{11}H_{11}NO_4S$; C, 52.17; H, 4.34, N, 5.33; $[\alpha]_D^{29}$=+4.00 (c 0.5, $CHCl_3$); IR (KBr): 3466 (br), 3241, 2922, 1765, 1627, 1451, 1331; ^{1}H NMR ($CDCl_3$) δ 3.2 (t, J=5 Hz, 1H, OH), 3.9 (s, 3H, $COOCH_3$), 4.15, 4.4 (m,m, 2H, $C^{\beta}H_2$), 5.4 (t, J=4 Hz, 1H, $C^{\alpha}H$), 7.4 (dd, J=8, 4 Hz, 1H), 7.6 (m, 2H), 8.1 (d, J=8 Hz, 1H) (aromatic); FAB MS (m/z) (%): 254 (100) $(MH)^+$, 276 (7) $(M+Na)^+$; Anal. Found: C, 51.56; H, 4.25; N, 5.24. Calcd for $C_{11}H_{11}NO_4S$: C, 52.17; H, 4.34; N, 5.53.

3.3.12. Compound 14. Benzisothiazolone: AA=Trp; yellow solid; yield: (25%); $[\alpha]_D^{29}$=−75.00 (c 1, $CHCl_3$); IR (neat): 3420 (br), 3357 (br), 2930, 1748, 1663, 1552, 1453, 1308, 1240; ^{1}H NMR ($CDCl_3$) δ 3.5 (m, 2H, $C^{\beta}H_2$), 3.74 (s, 3H, $COOCH_3$), 5.78 (m, 1H, $C^{\alpha}H$), 7.2, 7.35, 7.6, 8.1 (m,m,m,m, 4H, ArH); ^{13}C NMR ($CDCl_3$) δ 27.62 (C^{β}), 52.8 (C^{α}), 55.97 ($-OCH_3$), 110.12–141.19 (C aromatic), 165.92 (–COO), 170.69 (Ar-CO); FAB MS (m/z) (%): 353 (66) $(MH)^+$, 375 (11) $(M+Na)^+$, 705 (4) $(2M+H)^+$; Anal. Found: C64.31; H4.34; N, 7.80. Calcd for $C_{19}H_{16}N_2O_3S$: C, 64.77; H, 4.55; N, 7.95.

3.3.13. Compound 15. Benzisothiazolone: AA=His; yellow solid; yield: (56%; mp 240–242°C; IR (KBr): 3446 (br), 3025, 1650, 1455, 1340; ^{1}H NMR ($CDCl_3$–DMSO-d_6) δ 3.43 (m, 2H, $C^{\beta}H_2$), 3.75 (s, 3H, $COOCH_3$), 5.62 (m, 1H, $C^{\alpha}H$), 6.73 (br, Im 4H), 7.38 (br, 1H, Im 2H), 7.8 (br, Im NH); FAB MS (m/z) (%): 304 (100%) $(MH)^+$; Anal. Found: C, 55.55; H, 4.19; N, 14.21. Calcd for $C_{14}H_{13}N_3O_3S$: C, 55.45; H, 4.29; N, 13.86.

3.4. Preparation of 2,2′-dithiobis-[4′-(sulfamoyl)-benzanilide] (16)

To 2.58 g (14.99 mmol) of sulfanilamide in 50 mL of pyridine at 0–5°C was added in drops, 2 g (5.83 mmol) of 2,2′-dithiodibenzoyl chloride (**2**) in 20 mL of dry CH_2Cl_2. The mixture was stirred at 0–25°C for 18 h, filtered, the solid washed with 1N HCl (3×10 mL), water (3×10 mL), dried, suspended in a mixture of DMF (20 mL) and EtOH (25 mL), filtered and precipitated from the filtrate with 9 mL of 5% $NaHCO_3$. The product was collected by filtration, washed with water and then with EtOH and dried to afford 1.2 g of **16** (microcrystalline white powder).

Yield: 34%; mp 300°C (lit.[2a]; mp 311–312°C; IR (KBr): 3373, 3265, 1661, 1600, 1526, 1317, 1175; ^{1}H NMR ($CDCl_3$–DMSO-d_6) δ 7.1 (s, 4H, SO_2NH_2), 7.31–7.46 (m, 4H, ArH), 7.76–7.95 (m, 12H, ArH), 10.7 (s, 2H, NH); Anal. Found: C, 50.37; H, 3.57; N, 8.75. Calcd for $C_{26}H_{22}N_4O_6S_4$: C, 50.81; H, 3.58; N, 9.12.

3.4.1. 2,2′-Dithiobis [4′(sulfamido{Boc-Glu(γOMe)}) benzanilide] (17). A solution of Boc-Glu(γOMe)OH (0.836 g, 3.2 mmol) (prepared in two steps from Glu] in dry DMF (30 mL) was admixed with DCC (0.725 g, 3.52 mmol), left stirred for 5 min, admixed with

2,2′-dithiobis[4′-(sulfamoyl)benzanilide] (**16**) (0.984 g, 1.6 mmol) in dry DMF (10 mL) and the reaction left stirring for 48 h. Solvents were evaporated in vacuo, the residue dissolved in $CHCl_3$ (150 mL), filtered, the filtrate washed successively with cold saturated $NaHCO_3$ (2×15 mL), 1 M H_2SO_4 (2×15 mL), distilled water (1×10 mL), dried ($MgSO_4$) and chromatographed on silica gel using hexane/EtOAc (1:2) as eluent to afford 0.5 g of **17** and 0.7 g of unreacted **16** (yellow solid).

Yield: 98% (based on the starting material recovered); mp 113–115°C; $[\alpha]_D^{29}=-10.0$ (*c* 0.5, $CHCl_3$); IR (KBr): 3333, 2982, 1701, 1593, 1533, 1330, 1162; ^{1}H NMR ($CDCl_3$) δ 1.41 (s, 18H, BocCH_3), 1.67–2.10 (m, 4H, Glu C$^{\beta}H_2$), 2.32–2.35 (m, 4H, Glu C$^{\gamma}H_2$), 3.63 (s, 6H, $COOCH_3$), 4.34 (m, 2H, C$^{\alpha}$H), 5.13 (s, –SO_2–NH–CO–), 5.29 (d, *J*=2 Hz, 2H, BocNH), 7.5–7.85 (m, 16H, ArH), 8.3 (br, 2H, NH); FAB MS (*m*/*z*): 1123 $(M+Na)^+$; Anal. Found: C, 52.67; H4.57; N, 7.75. Calcd for $C_{48}H_{56}N_6O_{16}S_4$: C, 52.36; H, 5.09; N, 7.64.

3.5. The reaction of 2,2′-dithiodibenzoyl chloride with cystine-di-OMe: isolation of 18, 19 and 20

A solution of 2,2′-dithiodibenzoyl chloride (**2**) (1 g, 2.915 mmol) in dry CH_2Cl_2 (30 mL) and triethylamine (0.9 mL, 6.4 mmol) were added dropwise, simultaneously, to an ice cooled and stirred solution of cystine-di-OMe (generated in situ by the dropwise addition of triethylamine (0.9 mL, 6.4 mmol) to an ice cooled and stirred suspension of cystine-di-OMe·2HCl (1.1 g, 3 mmol) in dry CH_2Cl_2 (70 mL)). The reaction mixture was left stirred for 4 days at room temperature, washed successively with cold saturated $NaHCO_3$ (2×20 mL), 1 M H_2SO_4 (2×20 mL), distilled water (1×20 mL), dried ($MgSO_4$), evaporated under reduced pressure and chromatographed on silica gel. Elution with hexane/EtOAc (2:1) gave **18**, **19** and **20**.

3.5.1. Compound 18. Yellow unstable solid; yield: 3%; IR (neat): 3245, 2948, 1742, 1640, 1539, 1445, 1236; ^{1}H NMR ($CDCl_3$) δ 3.4 (d, *J*=5 Hz, 1H), 3.8 (d, *J*=5 Hz, 1H) (C$^{\beta}H_2$), 3.86 (s, 3H, $COOCH_3$), 4.2 (m, 2H, C$^{\alpha}$H), 7.36–7.85 (m, 4H, ArH); FAB MS (*m*/*z*) (%): 302 (34) $(MH)^+$, 324 (5) $(M+Na)^+$, 268 [M−SH], 236 [M−(S–S–H)].

3.5.2. Compound 19. Pale yellow thick prisms; yield: 17%; mp 150–152°C; IR (KBr): 3191, 2962, 1755, 1661, 1458, 1384; ^{1}H NMR ($CDCl_3$) δ 3.0 (dd, *J*=10, 5 Hz, 1H), 3.6 (dd, *J*=10, 3 Hz,1H) (C$^{\beta}H_2$), 3.78 (s, 3H, $COOCH_3$), 4.08 (m, 1H, C$^{\alpha}$H), 6.8 (br, 1H, NH), 7.4 (m, 2H), 7.6 (m, 1H), 7.7 (m, 1H) (ArH); FAB MS (*m*/*z*) (%): 238 (100) $(MH)^+$, 260 (4) $(M+Na)^+$, 475 (15) $(2M+H)^+$ (hydrogen bonded dimer), 497 (1) $(2M+Na)^+$; Anal. Found: C, 56.06; H, 4.70; N, 5.66. Calcd for $C_{11}H_{11}NO_3S$: C, 55.69; H, 4.64; N, 5.9.

3.5.3. Compound 20. Yellow powder; yield: 31%; mp 212–214°C; IR (KBr): 3279, 3063, 1742, 1640, 1539, 1337; ^{1}H NMR ($CDCl_3$) δ 3.55 (d, 4H, C$^{\beta}H_2$), 3.9 (s, 6H, $COOCH_3$), 4.94 (m, 2H, C$^{\alpha}$H), 6.1 (d, *J*=10 Hz, 2H, NH), 6.8 (dd, *J*=10, 0.5 Hz, 2H), 7.0 (dd, *J*=10 Hz, 2H), 7.6 (dd, *J*=10, 5 Hz, 2H), 8.1 (dd, *J*=10, 0.2 Hz, 2H) (ArH); FAB MS (*m*/*z*) (%): 539 (25) $(MH)^+$, 561 (6) $(M+Na)^+$; Anal. Found: C, 48.70; H, 4.08; N, 4.89. Calcd for $C_{22}H_{22}N_2O_6S_4$: C, 49.07; H, 4.08; N, 5.2.

3.6. Reaction of 2,2′-dithiodibenzoyl chloride with *o*-phenylene diamine: isolation of benzisothiazolone (21) and the 2+2 adduct (22)

To a stirred and ice-cooled mixture of *o*-phenylenediamine (0.157 g, 1.45 mmol) and triethylamine (0.45 mL, 3.2 mmol) in dry CH_2Cl_2 (40 mL) was added 2,2′-dithiodibenzoyl chloride (0.5 g, 1.457 mmol) in CH_2Cl_2 (20 mL) dropwise. The reaction mixture was left stirred at room temperature for 2 days, washed successively with cold saturated $NaHCO_3$ (2×15 mL), distilled water (1×15 mL), dried ($MgSO_4$), evaporated in vacuo and chromatographed on silica gel. Elution with hexane/EtOAc (1:1) afforded **21** and **22**.

3.6.1. Compound 21. Yellow solid; yield: 66%; IR (neat) 3434, 3336, 1681, 1635, 1504, 1458, 1334; ^{1}H NMR ($CDCl_3$) δ 2.83 (br, 2H, NH_2), 6.8 (m, 2H), 7.2 (m, 2H), (OPDA, H), 7.4 (dd, *J*=10, 5 Hz, 1H), 7.6 (dd, *J*=8, 4 Hz, 1H), 7.7 (dd, *J*=8, 4 Hz), 8.1 (d, *J*=8 Hz, 1H) (ArH); FAB MS (*m*/*z*) (%): 243 (100) $(MH)^+$, 485 (5) $(2M+H)^+$, 507 (1) $(2M+Na)^+$; Anal. Found: C, 64.12; H, 3.87; N, 11.75. Calcd for $C_{13}H_{10}N_2OS$: C, 64.46; H, 4.13; N11.57.

3.6.2. Compound 22. Pale yellow powder; yield: 5%; mp 215°C (dec); IR (KBr): 3472, 1662, 1605, 1526, 1451, 1315; ^{1}H NMR ($CDCl_3$–DMSO-d_6) δ 7.24–8.19 (m, 24H, ArH), 9.93–10.12 (brm, 4H, NH); FAB MS (*m*/*z*) (%): 757 (22) $(MH)^+$.

3.7. X-Ray diffraction analysis

The crystallographic parameters for the crystals are: (**9**) $C_{17}H_{15}NO_4S$, sp. gr. $P3_2$, $a=b=9.450(2)$ Å, $c=15.614(3)$ Å, $Z=3$, Mo rad., $R_1=0.101$; (**11**) $C_{12}H_{13}NO_4S$, sp. gr. $P2_12_12_1$, $a=9.705(2)$ Å, $b=10.181(2)$ Å. $c=12.433(3)$ Å, $Z=4$, Mo rad., $R_1=0.059$; (**12**) $C_{24}H_{28}N_2O_8S_2$, sp. gr. $P2_1$, $a=5.041(4)$ Å, $b=20.271(4)$ Å, $c=12.769(4)$ Å, $\beta=91.77(4)°$, $Z=2$, Cu rad., $R_1=0.097$, extremely fine needle crystal with 0.06×0.03 mm^2 cross-section; (**19**) $C_{22}H_{22}N_2O_6S_2$ (dimer), sp. gr. $P2_1/n$, $a=7.747(1)$ Å, $b=19.889(2)$ Å, $c=14.482(1)$ Å, $\beta=94.65(1)°$, $Z=4$ (dimer), Cu rad., $R_1=0.051$; (**21**) $C_{13}H_{10}N_2OS$, sp. gr. *Pbca*, $a=19.109(5)$ Å, $b=15.817(7)$ Å, $c=7.642(7)$ Å, $Z=8$, Mo rad., $R_1=0.056$.[12]

Acknowledgements

Financial assistance from Indian National Science Academy, New Delhi and Department of Biotechnology, New Delhi is gratefully acknowledged, as well as the Office of Naval Research, USA and NIH grant 30902.

References

1. (a) Demene, H.; Dong, C. Z.; Ottmann, M.; Rouyez, M. C.; Jullian, N.; Morellet, N.; Mely, Y.; Darlix, J. L.; Fournie-Zaluski, M. C.; Saragosti, S.; Roques, B. P. *Biochemistry* **1994**, *33*, 11707–11716. (b) South, T. L.; Summers, M. F. *Protein Sci.* **1993**, *2*, 3–19. (c) Delahunty, M. D.; South,

T. L.; Summers, F.; Karpel, R. L. *Biochemistry* **1992**, *31*, 6461–6469.

2. (a) Domagala, J. M.; Bader, J. P.; Gogliotti, R. D.; Sanchez, J. P.; Stier, M. A.; Song, Y.; Vara Prasad, J. V. N.; Tummino, P. J.; Scholten, J.; Harvey, P.; Holler, T.; Gracheck, S.; Hupe, D.; Rice, W. G.; Schultz, R. *Bioorg. Med. Chem.* **1997**, *3*, 569–579. (b) Tummino, P. J.; Scholten, J. D.; Harvey, P. J.; Holler, T. P.; Maloney, L.; Gagliotti, R.; Domagala, J.; Hupe, D. *Proc. Natl Acad. Sci. USA* **1996**, *93*, 969–973. (c) Rice, W. G.; Turpin, J. A.; Shaeffer, C. A.; Graham, L.; Clanton, D.; Buckheit, Jr., R. W.; Zaharevitz, D.; Summers, M. F.; Wallqvist, A.; Covell, D. G. *J. Med. Chem.* **1996**, *39*, 3606–3616. (d) Rice, W. G.; Supko, J. G.; Malspeis, L.; Buckheit, Jr., R. W.; Clanton, D.; Bu, M.; Graham, L.; Schaeffer, C. A.; Turpin, J. A.; Domagala, J.; Gogliotti, R.; Bader, J. P.; Halliday, S. M.; Coren, L.; Sowder II, R. C.; Arthur, L. O.; Henderson, L. E. *Science* **1995**, *270*, 1194–1197. (e) Loo, J. A.; Holler, T. P.; Sanchez, J.; Gogliotti, R.; Maloney, L.; Reily, M. D. *J. Med. Chem.* **1996**, *39*, 4313–4320.
3. (a) Ranganathan, S.; Jayaraman, N.; Chatterji, D. *Biopolymers* **1997**, *41*, 407–417. (b) Ranganathan, S.; Jayaraman, N.; Roy, R.; Madhusudanan, K. P. *Tetrahedron Lett.* **1993**, *34*, 7801. (c) Ranganathan, S.; Jayaraman, N. *Tetrahedron Lett.* **1992**, *33*, 6681–6682. (d) Ranganathan, S.; Jayaraman, N.; Roy, R. *Tetrahedron* **1992**, *48*, 931–938.
4. (a) Ranganathan, S.; Jayaraman, N. *J. Chem. Soc., Chem. Commun.* **1991**, 934–935. (b) Chaudhuri, A. *Curr. Sci.* **1995**, *68*, 692–698.
5. (a) Klug, A. *J. Mol. Biol.* **1999**, *293*, 215–218. (b) Kamiuchi, T.; Abe, E.; Imanishi, M.; Kaji, T.; Nagaoka, M.; Sugiura, Y. *Biochemistry* **1998**, *37*, 13827–13834. (c) Berg, J. M.; Shi, Y. *Science* **1996**, *271*, 1081–1085. (d) Klug, A.; Schwabe, J. W. R. *FASEB* **1995**, *9*, 597–603. (e) Berg, J. M. *Acc. Chem. Res.* **1995**, *28*, 14–19. (f) Suzuki, M.; Gerstein, M.; Yagi, N. *Nucleic Acids Res.* **1994**, *22* (16), 3397–3405.
6. (a) Crescenza, A.; Botta, M.; Corelli, F.; Santini, A.; Tafi, A. *J. Org. Chem.* **1999**, *64*, 3019–3025. (b) Fotsch, C.; Kumaravel, G.; Sharma, S. K.; Wu, A. D.; Gounarides, J. S.; Nirmala, N. R.; Peter, R. C. *Bioorg. Med. Chem. Lett.* **1999**, *9*, 2125–2130.
7. (a) Mooney, R. A.; Laudick, R. *Cell* **1999**, *98*, 687–690. (b) Zhang, G.; Campbell, E. A.; Minakhin, L.; Richter, L.; Severinov, K.; Darst, S. A. *Cell* **1999**, *98*, 811–824.
8. Enzyme aliquots containing 0.4 μM of *E. coli* RNA polymerase (5 μL from 4 μM stock) in 5 μL of 1×transcription buffer (1×transcription buffer: 50 mM Tris·HCl (pH 7.8), 0.1 mM EDTA, 0.1 mM DTT, 50 mM NaCl, 3 mM $Mg(OAc)_2$, BSA 25 mg/mL), after admixing with 0.8 μM solution of either dithiobisbenzamides or benzisothiazolones (5 μL from 8 μM stock in methanol) and 35 μL of MilliQ water was incubated for 15 min, dialyzed overnight (Dialysis buffer: 10 mM Tris·HCl (pH 8), Glycerol 5% (v/v), 0.1 mM EDTA, 0.1 mM DTT, 50 mM NaCl), and 20 μL of the treated and dialyzed enzyme mixed with 10 μL of 4×trancription assay mixure (1×transcription assay mixture: 40 mM Tris·HCl (pH 8), 10 mM $MgCl_2$, 1 mM EDTA, 16 mM βME, 0.2 mM ATP, 0.2 mM CTP, 0.2 mM GTP, 0.05 mM UTP, 50 mM ^{3}H UTP, Calf thymus DNA, 1 mg/mL. The solution was made up using milliQ water) and 10 μL of MilliQ water. The mixture was incubated for 20 min, and spotted on to a DE81 filter paper strip, which was precoated with EDTA to arrest further transcription. The filter paper strips were allowed to air dry for 3 h, washed successively with 5% Na_2HPO_4 solution (3×200 mL, 10 min each), distilled water (2×200 mL, 5 min each), and then with ethanol (2×75 mL). These strips were then dried under an IR lamp, put in the scintillation fluid and scintillation count was noted. The count given by the native enzyme was taken as 100% and the relative value shown by the inhibited enzyme gave the percentage loss of activity.
9. Mayalagu, S.; Patturajan, M.; Chatterji, D. *Gene* **1997**, *190*, 77–85.
10. Markov, D.; Naryshkina, T.; Mustaev, A.; Severinov, K. *Genes Dev.* **1999**, *13*, 2439–2448.
11. The conformations of cyclic, **20** and the open analog **3** have been studied using simulated annealing molecular dynamics. Initial profiles were developed based on the diphenyldisulphide conformations found in the Cambridge Structural Database. In the lowest energy conformation thus derived the disulfide linkage was inaccessible because of it being buried. In the open analogue **3**, similar studies suggested an open access to the disulfide bridge involved in the exchange.
12. Crystallographic data for the structures reported, have been deposited as supplementary publication nos. CCDC 175203 (**12**), CCDC 175204 (**19** dimer), CCDC 17611 (**9**), CCDC 17612 (**11**), CCDC 17613 (**21**) at the Cambridge crystallographic Data Center. Copies of the data can be obtained free of charge on application to the Director, CCDC, 12 Union Road, and Cambridge CB2 1EZ, UK (fax: +44-1223-336-033; e-mail: deposit@cdc.cam.ac.uk).